INFLUENCE OF CONTINUITY ON PUNCHING RESISTANCE AT EDGE COLUMNS

Soares LFS[a] and Vollum RL[b]

Department of Civil and Environmental Engineering

a) Imperial College London, London SW7 2AZ, United Kingdom / CNPq – Science Without Borders
b) Imperial College London, London SW7 2AZ, United Kingdom

Corresponding author: Dr Robert L Vollum

Department of Civil and Environmental Engineering

Imperial College London, London SW7 2AZ, United Kingdom

Email: r.vollum@imperial.ac.uk

Phone +44 (0)20 75945992

Fax: +44(0)20 75945934

Abstract

The paper considers punching failure at edge columns of reinforced concrete flat slabs without shear reinforcement and unbalanced moments about an axis parallel to the slab edge. Edge column punching shear tests have been carried out on a variety of isolated and continuous specimens. The influence of eccentricity and continuity on punching resistance is assessed using existing experimental data, nonlinear finite element analysis (NLFEA) and the Critical Shear Crack Theory (CSCT) as implemented in fib Model Code 2010 (MC2010). Relating punching resistance to the elastic unbalanced moment as done in MC2010 Levels I to III is shown to be overly conservative for continuous slabs. The ACI 318 and Eurocode 2 (EC2) practice of making the design punching resistance independent of the unbalanced moment is reviewed and shown to be reasonable particularly for continuous slabs.

NOTATION

A_{sl} area of flexural reinforcement

b_0 ACI 318 critical punching perimeter

b_e effective width of flexural reinforcement for normal moment at edge column

b_1, b_2 dimensions of critical section b_0 measured parallel and perpendicular to slab edge

b_{sr} width of support strip

b_u diameter of a circle with the same surface area as enclosed by the control perimeter

β enhancement factor for eccentric shear

c_1, c_2 column dimensions perpendicular and parallel to the slab edge

d average slab effective depth

d_n effective depth of top reinforcement normal to slab edge

d_g maximum aggregate size

e support eccentricity with respect to column axis

e' eccentricity of V with respect to the centroid of control perimeter

E_c concrete modulus of elasticity

E_s reinforcement modulus of elasticity

f_c compressive strength of concrete

f_y yield strength of reinforcement (subscript d for design)

γ_c, γ_s partial factors for concrete and steel

γ_v proportion of unbalanced moment transmitted by uneven shear

γ_f proportion of unbalanced moment transmitted by flexure

h slab thickness

J_c polar moment of inertia of critical section

k size effect factor

k_{dg} effectiveness coefficient dependent on maximum aggregate size

k_e effectiveness coefficient for eccentric shear

k_ψ coefficient relating shear resistance to slab rotation

L span between column centrelines

m_R nominal moment capacity per unit width

m_s average bending moment per unit width in support strip

M_{cf} bending moment across panel width at inner column face

M_{flex} moment of resistance of slab column connection at column face

M_{test} experimental ultimate bending moment about column centreline

M bending moment about column centreline

M_{cg} bending moment about centroid of critical section

M_{tmax} maximum unbalanced moment due to flexure

ρ flexural reinforcement ratio $\rho = \sqrt{\rho_{xl}\rho_{yl}}$

ρ_{xl}, ρ_{yl} flexural reinforcement ratio in x, y direction

ρ_{span} longitudinal flexural reinforcement ratio in span

ρ_{sup} flexural reinforcement ratio perpendicular to slab edge over width $b_e = c_2+2c_1$ centred on column

r_s position where radial bending moment is zero with respect to the column axis

u_1 length of EC2 control perimeter

u_{1*} length of reduced EC2 control perimeter

v_c punching shear resistance provided by concrete

v shear stress

V shear force

V_c punching resistance provided by concrete

V_{shear} calculated punching resistance

V_{flex} column load corresponding to flexural failure at inner column face

V_{Ro} punching resistance in absence of unbalanced moment

V_{test} experimental column load at failure

y perpendicular distance from slab edge to inner column face

ψ slab rotation outside critical shear crack

Introduction

There is no generally accepted theoretical treatment of punching shear and design methods are calibrated largely with data from tests on isolated internal slab column specimens. Punching at edge columns is much less researched than at internal columns despite the fact that buildings typically have more edge than internal columns. Furthermore, practical experience shows that design for punching shear is frequently more critical at edge than internal columns.

Significant investigations into the strength of slab edge column connections without shear reinforcement have been carried out by amongst others Zaghlool (1971) (8 isolated 1830×965×152 mm slabs with various column sizes), Stamenković & Chapman (1974) (6 isolated 914.4×914.4×76.2 mm slabs with 127 mm square columns), Regan et al. (1979) (21 tests on continuous slabs with thickness ranging between 80 mm and 125 mm), Regan (1993) (10 tests on 5 continuous 200 mm thick slabs), Rangan (1990) (4 continuous specimens with slab thickness of 80 mm and 100 mm), El-Salakawy et al. (1998) (2 isolated 1540×1020×120 mm slabs with 250 mm square columns) and Sherif et al. (2005) (5 isolated 1000×1200×120 mm slabs with various column sizes). As noted, these tests were carried out on a variety of isolated and continuous specimens of which the test arrangements of El-Salakawy et al. (1998) and Regan (1993) shown in Figure 1 are representative. The loading eccentricity is typically fixed in tests on isolated specimens but varies with loading in continuous specimens which are most representative of flat slabs. It is notable that of the 56 tests listed above, 38 were on slabs with thickness of 120 mm or less, 8 on 152 mm thick slabs and only 10 (Regan, 1993) on 200 mm thick slabs. This is significant due to the "size" effect which causes the shear stress at failure of geometrically similar specimens to reduce with increasing slab depth. Only slabs with thickness of 120 mm or greater are considered in the strength assessments of this paper due to difficulties in assessing the contribution of the size effect to the strength of thinner slabs.

Stamenković and Chapman (1974) were amongst the first to systematically examine the interaction of punching and flexure at internal, edge and corner connections. They found the interaction to be almost linear at internal connections and edge connections when the axis of the unbalanced moment is perpendicular to the slab edge. Significantly, they found the interaction to be almost square for "normal" moments where the axis of the unbalanced moment is parallel to the slab edge. Subsequently, Regan (1981, 1999) and Moehle (1988)

determined conditions under which the interaction between normal bending and punching can be neglected at edge columns. Their recommendations form the basis of the design provisions for punching at edge columns in EC2 (BSI, 2004) and ACI 318 (ACI, 2014) respectively. The most recent international design guidance on punching is found in MC2010 (fib, 2013) which is based on the Critical Shear Crack Theory (CSCT) (Muttoni, 2008). Unlike ACI 318 and EC2, MC2010 relates punching resistance at edge columns with normal moments to the eccentricity of the shear force. The paper examines the case for neglecting the interaction between punching resistance and unbalanced moments in design as well as the influence of flexural continuity on punching resistance.

Design methods for punching at edge columns in EC2, ACI 318-14, and MC2010

EC2 (BSI, 2004)

The design philosophy of EC2 for punching at edge columns with normal moments is based on the work of Regan (1981, 1999) who proposed the idealised moment-shear (*M*-*V*) interaction diagram shown in Figure 2 for punching at edge columns subject to normal unbalanced moments. The unbalanced moments in Figure 2 are calculated relative to the column centreline. According to Regan (1981), the total moment at the inner column face M_{cf} is made up of a "component M_f resisted by steel passing through the column face and two components each M_t resisted by steel distributed within a width r on either side of the column. The components M_t are eventually transmitted to the column through torsion on its side faces". Regan (1981) showed that for practical purposes, the width r can be taken as the perpendicular distance y from the slab edge to the inner column face. The increment from points C to B in bending moment in Figure 2 is due to eccentric shear. The maximum shear resistance occurs at point A which corresponds to uniform shear at the column faces in contact with the slab (Regan, 1999). According to Regan (1999), design for punching in flat

slabs can normally be based on point B in Figure 2 since tests on statically indeterminate flat slabs specimens indicate complete or nearly complete development of flexural capacity at punching failure.

In EC2, the design shear stress is given by:

$$v = \beta \frac{V}{u_1 d} \qquad (1)$$

where the multiple β accounts for the effects of uneven shear, d is the average effective depth of the tension reinforcement and u_1 is the basic control perimeter which is located at $2d$ from the column face. Where the eccentricity perpendicular to the slab edge is toward the interior and there is no eccentricity parallel to the edge, EC2 considers shear stress to be uniformly distributed along the reduced control perimeter u_1^* depicted in Figure 3. This is equivalent to taking β as u_1/u_1^* in equation (1) and is intended to limit the maximum design shear force to the resistance at point B in Figure 2 which eliminates the need to consider interaction between punching and unbalanced moment. EC2 calculates the concrete contribution to punching shear resistance as follows:

$$v_c = 0.18(100\rho f_c)^{\frac{1}{3}}(1 + (200/d)^{0.5})/\gamma_c \qquad (2)$$

where $\rho = \left(\rho_{xl}\rho_{yl}\right)^{0.5} \leq 0.02$ in which ρ_{xl} and ρ_{yl} are the flexural tension reinforcement ratios $\frac{A_{sl}}{bd}$ within a slab width equal to the column plus $3d$ to each side. f_c is the characteristic concrete cylinder strength, d is the average effective depth of the tension reinforcement and γ_c is the partial factor for concrete which equals 1.5 for design.

EC2 requires the bending moment at the column face M_{cf} to be resisted by reinforcement centred on the column within a width c_2+y where y is the perpendicular distance from the inner column face to the slab edge. However, it is common UK practice

(The Concrete Society, 2007; IStructE, 2006) to provide flexural reinforcement within $b_e = c_2 + 2y$ and to limit M to $M_{tmax} = 0.255(c_2 + y)f_c d_n^2/\gamma_c$ (where d_n is the effective depth of top reinforcement normal to the slab edge and γ_c = 1.5) as required by Annex I (informative) of EC2 to prevent reinforcement congestion.

ACI 318-14

ACI 318-14 (ACI, 2014) adopts a rectangular control perimeter of length b_0 which is located at a distance $0.5d$ from the perimeter of the concentrated load. The maximum shear stress is calculated as the greatest of:

$$v_{(AB)} = \frac{V}{b_0 d} + \frac{\gamma_v M_{cg} c_{AB}}{J_c}$$

$$v_{(CD)} = \frac{V}{b_0 d} - \frac{\gamma_v M_{cg} c_{CD}}{J_c} \qquad (3)$$

where J_c is a property of the critical section analogous to polar moment of inertia which is defined by MacGregor and Wight (2005) for edge column connections. The dimensions c_{AB} and c_{CD} are depicted in Figure 4 which also shows the stress distribution on the critical section. A proportion $\gamma_f M_{cg}$ of the unbalanced moment about the centroid of the critical perimeter is assumed to be resisted by flexure with the remainder $\gamma_v M_{cg}$ resisted by eccentric shear where $\gamma_v = 1 - \gamma_f$ is given by:

$$\gamma_v = 1 - \frac{1}{1 + \left(\frac{2}{3}\right)\sqrt{b_1/b_2}} \qquad (4)$$

where b_1 and b_2 are the dimensions of the critical section b_0 measured parallel and perpendicular to the slab edge

On the basis of research by Moehle (1988), ACI 318-14 allows γ_v to be taken as 0 for edge columns with unbalanced moments about an axis parallel to the slab edge provided $V \leq$

$0.75V_{R0}$ (where V_{R0} is the shear resistance in the absence of unbalanced moment) and sufficient flexural reinforcement is provided within a width of c_2+3h, centred on the column to resist M_{cg}. Taking $\gamma_v = 0$ and limiting the design shear resistance to $0.75V_{R0}$ is equivalent to taking $\beta = u_1/u_1^*$ in EC2. The safety of this practice is questioned by Ghali et al. (2015).

MC2010

MC2010 (fib, 2013) relates punching resistance to the rotation in the so called critical shear crack. It locates the basic control perimeter u at a constant distance of $0.5d$ from the column face. MC2010 has four levels of approximation of which I to III are intended for design and IV for assessment. Level II is intended for standard design unless the geometry is irregular in which case Level III is required. The shear resistance is calculated in terms of the slab rotation ψ relative to the column which is calculated in Levels II and III as follows:

$$\psi = \alpha \frac{r_s}{d} \frac{f_{yd}}{E_s} \left(\frac{m_s}{m_R}\right)^{1.5} \quad (5)$$

where r_s denotes the position where the radial bending moment is zero with respect to the column axis, m_s is the average design moment for the reinforcement moment per unit width in the support strip, which is of width $b_{sr} = c_1+2y$ for normal moments at edge columns, and m_R is the design average flexural strength per unit width of the support strip. The coefficient α in equation (5) is 1.5 for Level II and 1.2 for Level III. In Level II, r_s is estimated as $0.22L$ where L is the slab span and the design moment for the reinforcement m_s normal to the slab edge is estimated as:

$$m_s = V\left(\frac{1}{8} + \frac{e'}{b_{sr}}\right) \quad (6)$$

where e' is the eccentricity of V with respect to the centroid of the control perimeter.

In Level III, both m_s and r_s are calculated with linear elastic finite element analysis (LFEA) but r_s should not be taken as less than $0.67b_{sr}$ at edge and corner columns. Although

not stated in MC2010, the reinforcement should be designed for the Wood moments (Wood, 1968) or equivalent. MC2010 bases the shear resistance on the greater of the rotations about axes normal and parallel to the slab edge. The punching resistance provided by the concrete is calculated as:

$$V_c = k_\psi k_e \frac{\sqrt{f_c}}{\gamma_c} ud \tag{7}$$

in which f_c is in MPa, d is the average effective depth of the tension reinforcement which is assumed to equal the shear resisting effective depth in this paper and k_e is a reduction factor for eccentric shear. MC2010 permits k_e to be estimated as 0.7 for braced frames where the adjacent spans do not differ in length by more than 25%. MC2010 also calculates k_e as follows:

$$k_e = 1/(1 + \frac{e\prime}{b_u}) \tag{8}$$

where *e'* is the eccentricity of *V* with respect to the centroid of the basic control perimeter *u*, and b_u is the diameter of a circle with the same surface area as enclosed by *u*.

Additionally, k_e can be determined from LFEA as the ratio of the average to peak shear stress (v_{ave}/v_{max}) on the basic control perimeter. This is equivalent to assuming punching failure occurs when the peak stress on the control perimeter reaches the shear resistance.

The parameter k_ψ depends on the slab rotation and is calculated as:

$$k_\psi = \frac{1}{1.5 + 0.9 k_{dg} \psi d} \leq 0.6 \tag{9}$$

$$k_{dg} = \frac{32}{16 + d_g} \geq 0.75 \tag{10}$$

where d_g is the maximum aggregate size.

Interaction between punching resistance and unbalanced moment

The interaction between punching resistance and unbalanced moment is assessed in Figure 5 using the data in Table 1 which includes all the slabs considered by Moehle (1988) with depths of at least 120 mm not subject to inelastic load reversals. Figure 5 shows the interaction between M_{cf}/M_{flex} and V_{test}/V_{shear} where M_{cf} is the ultimate bending moment across the panel width at the inner column face, M_{flex} is the moment of resistance of the slab column connection at the column face, V_{test} is the measured punching strength and V_{shear} is the punching resistance calculated with EC2 using its reduced perimeter u_1*. M_{flex} is calculated assuming reinforcement to be effective if placed within an effective width of $b_e = c_2+2y$ as commonly adopted in UK practice (IStructE, 2006) and is limited to a maximum of $M_{tmax} = 0.255(c_2 + y)f_c d_n^2/\gamma_c$ in accordance with Annex I of EC2. M_{cf} was calculated from statics assuming the support reaction to be linearly distributed around the simply supported edges of the isolated test specimens. Although approximate, FEA shows this procedure to be reasonable. The development of M_{flex} at the column face does not lead to flexural collapse of continuous slabs if the span reinforcement is still elastic. However, all the slabs in Table 1 are reported as failing in punching, typically subsequent to yielding of flexural reinforcement at the column face. Consequently, all the points in Figure 5 correspond to punching failure. Figure 5 shows that although punching resistance reduces with eccentricity, the design punching resistance can be safely assumed to be independent of eccentricity if limited by M_{flex}. Table 1 shows M_{cf}/M_{flex} and M/M_{flex} for M_{flex} calculated with $b_e = c_2+2y$ omitting the EC2 Annex I limit on M_{tmax} without which EC2 overestimates the strength of Hawkins and Corley's (1974) specimen CN1. Cases where the punching resistance is calculated to have been limited by flexure at the column face are highlighted in bold. There are no significant differences between the punching resistances of isolated and continuous specimens evident in

Figure 5 which suggests that it is unnecessary to differentiate between the two types of specimen when evaluating test data.

Numerical investigation

Nonlinear finite element models were developed of two isolated slabs tested by El-Salakawy et al. (1998) and five continuous slab tests of Regan (1993). These tests were chosen because they were highly instrumented with reinforcement strains and rotations being measured. Details of the specimens are given in Figure 1 and Table 1.

The objective of the NLFEA was to gain insight into i) the shear stress distribution in the slab around the ACI 318 critical section, ii) the proportion of unbalanced moment resisted by eccentric shear and iii) the influence of flexural continuity on punching resistance. The main difference between isolated and continuous edge column punching tests is that the eccentricity *M/V* is typically constant in tests on isolated specimens but varies with load in continuous specimens due to redistribution of bending moment between the span and support. The influence of flexural continuity on punching resistance is investigated in a parametric study of specimens geometrically similar to those tested by Regan (1993). The studies investigate the influences of i) redistributing reinforcement between the span and support and ii) providing surplus flexural reinforcement. Comparisons are made between the punching resistances given by NLFEA, EC2, and MC2010.

Material modelling

The NLFEA was carried out with Diana 9.6 (TN0, 2014). Concrete was modelled with the 'total strain fixed crack model' in Diana which evaluates the stress-strain relationship in the directions of the principal axes at first cracking which is governed by a tension cut-off criterion. The fracture energy based Hordijk (1991) model was used to

simulate concrete tensile behaviour after cracking. The Thorenfeldt model (Thorenfeldt et al., 1987) was used for concrete in compression in conjunction with the four-parameter Hsieh-Ting-Chen (Chen, 1982) failure surface which models the increase in concrete compressive strength with increasing isotropic stress. The reduction in concrete compressive strength due to lateral cracking was modelled following Vecchio and Collins (1993). After cracking, the shear stiffness was reduced by a constant shear retention factor of 0.1 on the basis of a sensitivity study. The concrete elastic modulus E_c and tensile fracture energy G_f were calculated in accordance with fib Model Code 1990 (CEB-FIP, 1993) as $E_c = 10{f_c}^{1/3}$ kN/mm^2 and $G_f = 0.025(f_c/10)^{0.7}$ Nmm/mm^2. Measured concrete tensile strengths were used. The reinforcement was modelled with fully bonded embedded reinforcement bars which do not have degrees of freedom of their own.

Isolated slabs of El-Salakawy et al.

El-Salakawy et al. (1998) tested two isolated punching specimens, without shear reinforcement, depicted XXX and HXXX with geometry and loading arrangement as shown in Figure 1. The concrete cylinder strengths of XXX and HXXX were similar at 33 MPa and 36.5 MPa respectively. The tensile strengths were 3.38 and 3.36 MPa respectively. The height of the column above and below the slab was 700 mm. The average tension reinforcement ratio was 0.0075 parallel and perpendicular to the long edge using 11.3 mm diameter bars. The average compression reinforcement ratio equalled 0.0045 in both directions using 7 mm diameter bars. The M/V ratio about the column centreline was 0.3 m for XXX and 0.66 m for HXXX.

The slab, column and steel plates were modelled with twenty-node isoparametric solid elements as shown in Figure 6. The mesh size was chosen on the basis of a sensitivity study. Eight rows of solid elements were provided through the slab thickness with plan dimensions

of 50×50 mm. A 3 × 3 × 3 integration scheme was adopted for solid elements. The mid-surface of the slab was meshed with non-structural composed elements in order to obtain the generalised moment and force distribution within the slab. The reinforcement was modelled with embedded bars assuming perfect bond.

Influence of eccentricity

The NLFEA gave very good estimates of the measured deflections as shown in Figure 7 for XXX. Once the NLFEA was validated a parametric study was carried out to determine the effect of loading eccentricity on the punching resistance of XXX. Eccentricities *M/V* of 0.2 m, 0.3 m (XXX), 0.4 m, 0.5 m, 0.6 m and 0.66 m (HXXX) were modelled. The concrete properties of XXX were used except for *M/V* = 0.66m where the properties of HXXX were adopted. The results of the analyses were used to evaluate the MC2010 punching shear provisions at edge columns. According to MC2010, punching resistance is governed by the maximum rotation ψ of the slab relative to the column about the two principal axes of the slab. The critical axis is parallel to the slab edge for the analysed specimens. Figures 8a to d compare the following rotations for representative eccentricities:

1. Test data for XXX and HXXX;
2. NLFEA used for MC2010 Level IV (LIV);
3. MC2010 Level II (LII) with m_s from equation (6);
4. MC2010 Level III (LIII) with m_s and r_s from LFEA with shell elements;

Figure 8 also shows shear resistances calculated in accordance with MC2010 with the reduction factor for eccentric shear k_e given by:

5. $k_e = 0.7$;
6. Equation (8);
7. $k_e = v_{ave}/v_{max}$ with v_{ave} and v_{max} from LFEA.

Figures 8b and d show reasonable agreement between the measured and NLFEA rotations and failure loads particularly for XXX. The MC2010 failure load is given by the intersection of the resistance and rotation curves. Figure 8 shows that the resistances calculated with k_e from LFEA above are similar but slightly less than those with k_e from equation (8). Equation (5) gives reasonable estimates of rotation up to near failure if m_s is calculated with LFEA (LIII) but rotations are significantly overestimated if m_s is calculated with equation (6) (LII).

Figure 9 shows the influence of eccentricity on failure loads calculated with NLFEA, EC2 and MC2010 Levels II to IV. The Level IV resistances were calculated with NLFEA rotations and k_e from 5) to 7) above. The Level IV resistances are closest to the test and NLFEA results when calculated with k_e = 0.7. The Level III and IV predictions with k_e from equation (8) are similar and reasonable but Level II is overly conservative. Consideration of Figure 8 shows that Level III is less conservative than Level IV if k_e = 0.7. According to EC2, the failure load is the least of V_{shear} calculated using u_1^* and V_{flex} which is calculated in Figure 9 assuming that M_{cf} equals M_{flex} calculated with $b_e = c_2+2y$. EC2 is seen to give conservative estimates of the strengths of XXX and HXXX, when limited by M_{flex} at the column face, and is considerably simpler to implement than MC2010.

Investigation of shear forces on ACI 318 critical section

Both MC2010 and ACI 318 allow punching resistance to be calculated on the basis that failure occurs when the peak shear stress reaches the available shear resistance. MC2010 allows the peak shear stress to be determined with linear FEA whereas ACI 318 calculates the peak shear stress using equation (3). This section compares the shear stresses given on the ACI 318 critical perimeter by NLFEA and ACI 318. For each analysis, shear forces per unit length and the proportion of unbalanced moment resisted by eccentric shear γ_v were

calculated on the ACI 318 critical section, at the NLFEA failure loads, with i) NLFEA, ii) LFEA with solid elements and iii) LFEA with shell elements. Figure 10a shows the variation in γ_v with eccentricity given by i) to iii) above and γ_v from equation (4). Significantly, equation (4) underestimates the proportion of unbalanced moment resisted by eccentric shear which is greatest for the NLFEA as found by Gayed and Ghali (2008) who concluded that ACI 318 is incorrect to allow $\gamma_v = 0$. Conversely, the authors consider taking $\gamma_v = 0$ when $V \leq 0.75V_{R0}$ to be a computational device equivalent to the EC2 practice of taking β as u_1/u_1* in equation (1) which is supported by Figure 5 providing sufficient flexural reinforcement is placed within $b_e = c_2+2y$ to resist the unbalanced moment at the column face and $M_{cf} \leq 0.255(c_2 + y)f_c d_n^2/\gamma_c$.

Figures 10b and 10c show shear force distributions along the ACI 318 critical section in N/mm for XXX and HXXX respectively. The shear forces were derived using linear elastic FEA with both shell elements and brick elements as well as NLFEA with brick elements. The FEA shear forces in Figure 10 are averages between adjacent nodes on plan which are at 25 mm centres. Averaging was carried out to smooth the shear force distribution and reduce the calculated shear force at the slab edge which is mesh sensitive and overestimated by FEA. Physically, the averaging width of 25 mm is approximately ¼ of the average effective depth d. The peak shear forces per unit length given by FEA are seen to be model dependent suggesting that peak shear stress is not a good failure criterion. Figures 10b and 10c also show shear forces per unit length calculated using equation (3) with γ_v from i) equation (4) and ii) NLFEA. Both give peak shear forces less than given by FEA but greater than the resistance calculated in accordance with ACI 318. These observations are consistent with the conclusions of Moehle (1988) who suggested that the peak shear stress, which depends significantly on the method of calculation, is not a good measure of punching failure at edge columns.

Continuous specimens of Regan

Regan (1993) tested five full-scale continuous edge column punching shear specimens. The slabs were 200 mm thick, 3000 mm wide and 5784 mm long with 300 mm square columns at the centre of the short edges at each end as shown in Figure 1. The longitudinal flexural tension reinforcement ratio in the span was 0.5%. The flexural tension reinforcement ratio normal to the slab edge, within a width $b_e = 2c_1 + c_2$ centred on the column, ρ_{sup} was 0.8% in slabs S1 to S3, 1.0% in S4 end 1 and 0.5% in S4 end 2. The reinforcement ρ_{sup} was provided in the form of U bars and distributed over a width of 500 mm in slabs S1 to S3 and S4 end 2. In S4 end 1, ρ_{sup} was distributed over a width of 600 mm. No other longitudinal hogging reinforcement was provided within 500 mm of the column centreline. Further details of the slabs are summarised in Table 1 including the punching resistances V_{shear} calculated according to EC2. The two ends of each slab were tested separately, with the column providing the support at one end and the other end simply supported along a line just inside from the column face. The vertical loading arrangement was shown as in Figure 1b except the final loading stage of slab 3 end 1 where four equal loads were applied at the loading points closest to the supported column. At each loading stage equal and opposite horizontal forces were applied to the column at the end under test "so as to keep the column free of rotation" (Regan, 1993). In slabs S1 and S2, the transfer moments had become constant before punching occurred and the bottom steel yielded in the span. In slab S4 end 1 with increased ρ_{sup}, the span steel had not visibly yielded when punching occurred. Mid-span yield was well developed in slab S4 end 2 at punching failure.

Symmetry and a gradated mesh were used to reduce the number of elements, with the region around the connection being most refined as shown in Figure 11. Figure 12 compares the measured and predicted slab rotations relative to the column for slab 1 (f_{ct} = 3.36 MPa) end 1, slab 2 (f_{ct} = 3.14 MPa) ends 1 and 2 and slab 4 (f_{ct} = 3.5 MPa) ends 1 and 2. Rotations

are shown about an axis parallel to the 3000 mm slab edge as these were greatest and hence govern punching resistance according to MC2010. The NLFEA gives good predictions of the measured rotations and failure loads of the slabs. Figure 12 also shows rotations calculated for each test with MC2010 Levels II and III. The Level II rotations were calculated with the measured ultimate eccentricity M/V which is less than the elastic eccentricity which would be used in design. The MC2010 resistances with k_e from equation (8) are evaluated with both the measured ultimate eccentricity and the elastic eccentricity. The latter are almost identical to resistances calculated with k_e derived from LFEA with shell elements. The MC2010 failure loads are given by the intersection of the rotation and resistance curves in Figure 12. MC2010 Level IV, with rotations from the NLFEA, gives reasonable estimates of the measured punching resistances, but no better than EC2, if k_e = 0.7. However, resistances are underestimated if k_e is calculated with equation (8) even if the measured ultimate eccentricity is used. MC2010 Levels II and III significantly underestimate punching resistance particularly if k_e is calculated using the elastic eccentricity. The flexural failure loads in Figure 12 were calculated neglecting strain hardening and the width of loading plates assuming yielding in the span and an ultimate moment at the column face of M_{flex} calculated with $b_e = c_2+2y$.

Influence of reinforcement arrangement

A series of parametric studies were carried out to investigate the influence of varying the longitudinal flexural reinforcement in slabs with the same geometry as tested by Regan (1993). Analyses were carried out with longitudinal hogging reinforcement ratios ρ_{sup} within $b_e = 2c_1 + c_2$ at the column support equal to 0.43%, 0.8%, 1.0%, 1.2% and 1.6%. For each of these ratios, the longitudinal reinforcement ratio in the span ρ_{span} was taken as 0.25%, 0.5%, which corresponds to Regan's slabs, and 1.0%. The resulting load rotation diagrams are

shown in Figure 13a which also shows the punching resistance according to MC2010 with k_e = 0.7. Despite giving good strength predictions for the El-Salakawy et al. (1998) and Regan (1993) slabs, the NLFEA appears to overestimate the punching resistance of the slabs with 1.0% flexural reinforcement. However, the NLFEA rotations are considered reasonable prior to failure on the basis of good comparison with test results in Figures 8 and 12. These and other NLFEA validation studies (Soares and Vollum, 2015) indicate that rotations can be predicted more reliably than punching resistances highlighting the benefit of the rotation based failure criteria of MC2010. Figure 13a shows that the slab rotation relative to the column is largely governed by ρ_{span} and is almost independent of ρ_{sup}. This is significant because EC2 and MC2010 Levels I to III relate punching resistance to ρ_{sup} and not ρ_{span}. Figure 13b illustrates the influence of ρ_{sup} on punching resistance according to MC2010 Levels III and IV. Test results, normalised by $(35.4/f_c)^{1/3}$ in accordance with equation (2), are also shown for the Regan slabs considered in Figure 11 for which ρ_{span} = 0.5%. MC2010 Level IV compares favourably with the test results but Level III greatly overestimates the influence of ρ_{sup} on punching resistance. This is largely explained by Figure 13c which shows the variation in eccentricity *M/V* with *V* for selected analyses. Significantly, *M/V* is not constant as assumed in MC2010 Level III but reduces with increasing *V* due to moment being redistributed into the span once torsional cracking and yielding of flexural reinforcement occurs at the support. Furthermore, *M/V* is almost independent of ρ_{sup} for given ρ_{span}. The underestimate of resistance is compounded if k_e is calculated with equation (8) using the elastic eccentricity.

Conclusions

The paper investigates the influence of unbalanced moment and flexural continuity on punching resistance at edge columns. It is shown that the current ACI 318 and EC2 practice

of neglecting the interaction between unbalanced moment and punching resistance is reasonable if the unbalanced moment is limited to $M_{tmax} = 0.255(c_2 + y)f_c d_n^2/\gamma_c$ (where γ_c = 1.5) as required by Annex I (informative) of EC2. MC2010 gives reasonable estimates of punching resistance if rotations are calculated with NLFEA and k_e = 0.7 but significantly underestimates punching resistance at edge columns of continuous slabs if rotations are calculated using Levels II or III, which are intended for design, with the underestimate greatest when k_e is calculated with equation (8) or LFEA. The conservatism of MC2010 Levels II and III for continuous slabs largely arises because *M/V* reduces below its elastic value as the loading is increased to failure due to support moments being redistributed into the span. Significantly, MC2010 Level IV and NLFEA predict longitudinal span reinforcement to have a much greater influence on punching resistance at edge columns of flat slabs than hogging reinforcement normal to the slab edge at the column. This has important design implications because it calls into question the common practice of increasing the area of hogging reinforcement at slab edges to increase punching resistance. The peak shear stress on the control perimeter is shown to depend on the method of calculation and not to be a reliable indicator of punching failure. For practical purposes, the current EC2 design rules appear satisfactory and superior to MC2010 Level III for continuous slabs. However, MC2010 provides useful insights into the parameters influencing punching resistance.

Acknowledgements

This research was supported by the Science Without Borders Program, through the National Council for Scientific and Technological Development (CNPq), funded by the Brazilian Ministry of Science and Technology. The assistance of Dr N. G. B. Albuquerque and Emeritus Professor P. E. Regan in providing references used to develop Table 1 is gratefully acknowledged.

References

ACI Committee 318 (2014), Building Code Requirements for Structural Concrete and Commentary, American Concrete Institute, Farmington Hills, MI.

BSI (2004) EN 1992-1-1:2004, Eurocode 2, Design of Concrete Structures – Part 1-1: General Rules and Rules for Buildings. BSI, London.

CEB-FIP (1993) CEB-FIP Model Code 1990. Comité Euro-International du Béton.

Chen WF. (1982) Plasticity in reinforced concrete. New York: McGraw-Hill Co.

El-Salakawy E F, Polak MA, Soliman MH (1998) Reinforced Concrete Slab-Column Edge Connections with Shear Studs. Canadian Journal of Civil Engineering, **27(2)**: 338-348.

fib (2013) fib Model Code for concrete structures 2010. fédération international du béton, Lausanne, Switzerland.

Gayed RB, Ghali A (2008) Unbalanced Moment Resistance in Slab-Column Joints: Analytical Assessment. *Journal of Structural Engineering* **134(5)**: 859-864

Ghali A, Gayed RB, Dilger W (2015) Design of Concrete Slabs for Punching Shear: Controversial Concepts. *ACI Structural Journal*, **112(4)**: 505-514.

Hordijk DA (1991) Local Approach to Fatigue of Concrete. PhD thesis, Delft University of Technology, Delft, the Netherlands.

Hawkins NM, WG Corley (1974) Moment Transfer to Columns in Slabs with Shearhead Reinforcement. ACI Special Publication SP-42, Shear in Reinforced Concrete.

MacGregor JG, Wight JK (2005) Reinforced Concrete Mechanics and Design. 4th Edition, Prentice Hill.

Moehle J (1988) Strength of Slab-Column Edge Connections. *ACI Structural Journal* **85(1)**: 89-98.

Mortin JD, Ghali A (1991) Connection of Flat Plates to Edge Columns, *ACI Structural Journal*, **88(2)**: 191-198.

Muttoni A (2008) Punching shear strength of reinforced concrete slabs without transverse

reinforcement. *ACI Structural Journal* **105(4)**: 440–450.

Rangan BV (1990) Tests on Slabs in the Vicinity of Edge Columns. *ACI Structural Journal*, 87(6): 623-629

Regan PE, Walker PR, Zakaria KA A. (1979) Test of Reinforced Concrete Flat Slabs. *CIRIA Project RP 220*, School of the Environment Polytechnic of Central London, London, 217 p.

Regan PE (1981) Behaviour of reinforced concrete flat slabs. Ciria Report 89, London.

Regan PE (1993) Tests of Connections between flat slabs and edge columns. School of Architecture and Engineering, University of Westminster. London.

Regan PE (1999) Ultimate limit state principles in fib Bulletin 2 Structural concrete Volume 2 Basis of design, Lausanne.

Sherif A, Emara MB, Hassanein A, Abul Magd S (2005) Effect of the Column Dimensions on the Punching Shear Strength of Edge Column-Slab Connections. ACI Special Publication 232, Punching Shear in Reinforced Concrete Slabs: 175-192.

Sherif AG, Dilger WH (2000a) Punching Failure of Full-Scale High Strength Concrete Flat Slabs, Proceedings, International Workshop on Punching Shear Capacity of RC Slabs, Stockholm, TRITA-BKN: Bulletin 57, KTH, Stockholm, Sweden: 235-243.

Sherif AG, Dilger WH (2000b) Tests of Full-Scale Continuous reinforced Concrete Flat Slabs, ACI Structural Journal, **97(3)**: 455-467.

Soares LFS and Vollum RL (2015) comparison of punching shear requirements in BS8110, EC2 and MC2010, Magazine of Concrete Research, 67(24): 1315-1328.

Stamenković A, Chapman JC (1974) Local Strength at Column Heads at Flat Slabs Subjected to a Combined Vertical and Horizontal Loading. *Proceedings of the Institution of Civil Engineers*. Part 2 Research and Theory **57(2)**: 205-232.

The Institution of Structural Engineers (2006) Standard Method of Detailing Structural Concrete. London

The Concrete Society (2007) Guide to the Design and Construction of Reinforced Concrete Flat Slabs. Technical Report 64, Camberley ISBN 1-904482-33-3

Thorenfeldt E, Tomaszewicz A and Jensen JJ (1987) Mechanical properties of high-strength concrete and applications in design. In Proc. Symp. *Utilization of High-Strength Concrete* (Stavanger, Norway) (Trondheim), Tapir.

TNO Diana (2014) Finite-element Analysis User's Manual. Release 9.6. TNO Diana BV, Delft, The Netherlands.

Vecchio FJ and Collins MP (1993) Compression response of cracked reinforced concrete. Journal of Structural Engineering ASCE 119(12): 3590–610.

Wood RH (1968) The Reinforcement of Slabs in Accordance with a Pre-Determined Field of Moments. *Concrete* **2(2)**: 69-76

Zaghlool ERF (1971) Strength and Behavior of Corner and Edge Column-Slab Connections in Reinforced Concrete Flat Plates. PhD Thesis, Department of Civil Engineering, University of Calgary.

Table 1 – Database of Tests

Author	Slabs	Experimental									EC2		
		c_1 *mm*	c_2 *mm*	h *mm*	d *mm*	f_c *MPa*	f_y *MPa*	ρ^d %	V_{test} *kN*	M_{test} *kNm*	M_{cftest}/M_{flex} c_2+2y	M_{test}/M_{flex} c_2+2y	V_{test}/V_{shear}
El-Salakawy *et al.* (1998) Isolated	XXX	250	250	120	89	33.0	545	0.79	125	38	1.01	1.35	1.25
	HXXX	250	250	120	89	36.5	545	0.79	69	46	**1.35**	1.63	0.67
Hawkins and Corley (1974) Isolated	CN1	305	305	152	121	22.7	459	1.29	111	61	**0.81**	0.97	0.61
	DN1	305	203	152	121	22.6	425	1.38	101	55	**1.01**	1.21	0.58
Mortin & Ghali (1991) Isolated	JS1	254	254	152	122	43.2	421	0.75	141	60	**1.67**	2.10	0.79
	JS4	254	254	152	122	32.2	421	1.01	141	60	**1.29**	1.63	0.79
Sherif *et al.* (2005) Isolated	EX-S1	300	300	120	99	35.6	394	1.07	167	50	0.98	1.38	1.14
	EX-S2	225	225	120	99	31.7	394	1.07	155	47	1.23	1.72	1.25
	EX-S3	150	150	120	99	31.0	394	1.07	95	29	**1.13**	1.59	0.90
	EX-S4	265	150	120	99	31.0	394	1.07	150	45	1.19	1.68	1.26
	EX-S5	150	375	120	99	31.0	394	1.07	172	52	**1.34**	1.89	1.31
Zaghlool (1971) Isolated	Z-IV(1)	178	178	152	121	27.3	476	1.30	122	45	**0.94**	1.15	0.77
	Z-V(1)	267	267	152	121	34.3	474	1.30	215	85	0.98	1.27	1.08
	Z-V(2)	267	267	152	121	40.5	474	1.70	247	94	0.90	1.18	1.07
	Z-V(3)	267	267	152	117	38.7	475	2.08	268	104	0.82	1.07	1.15
	Z-V(4)	267	267	152	121	35.0	437	1.30	0	81	**1.31**	1.31	0
	Z-V(5)	267	267	152	121	35.2	476	1.30	279	0	0.19	0.00	1.39
	Z-V(6)	267	267	152	121	31.3	476	1.30	117	88	**1.10**	1.34	0.61
	Z-VI(1)	356	356	152	121	26.0	476	1.30	265	107	0.98	1.38	1.29
Regan *et al.* (1979) Continuous	SE1	300	200	125	98	35.7	480	1.03	198	40	0.60	0.99	1.52
	SE2	300	200	125	101	43.7	480	0.47	192	34	1.53	2.76	1.70
	SE4	200	300	125	98	27.4	480	1.03	152	31	0.49	0.80	1.27
	SE5	200	300	125	98	44.2	500	0.78	164	39	0.94	1.40	1.28
	SE6	200	300	125	99	32.0	500	0.57	149	28	1.03	1.77	1.42
	SE7	200	300	125	99	39.6	500	0.81	129	32	0.94	1.37	1.02
	SE8	300	100	125	98	41.6	480	0.88	136	34	0.88	1.30	1.15
	SE9	250	250	125	98	41.4	480	0.73	123	36	**1.59**	2.19	1.00
	SE10	250	250	125	98	40.7	480	0.73	114	36	**1.65**	2.21	0.93
	SE11	250	250	125	98	50.0	480	0.73	138	40	**1.74**	2.41	1.06
Regan[a] (1993) Continuous	1(1)	300	300	200	168	35.4	507	0.56	282	118	0.81	1.18	1.04
	1(2)	300	300	200	168	35.4	507	0.56	264	138	**1.03**	1.37	0.97
	2(1)	300	300	200	168	35.4	507	0.56	256	124	0.91	1.24	0.94
	2(2)	300	300	200	168	35.4	507	0.56	285	129	0.92	1.29	1.05
	3(1)	300	300	200	168	41.0	507	0.56	416	73	0.40	0.72	1.46
	3(2)	300	300	200	168	41.0	507	0.56	233	148	**1.16**	1.46	0.82
	4(1)	300	300	200	165	42.7	507	0.66	289	149	0.88	1.17	0.98
	4(2)	300	300	200	168	42.7	507	0.45	281	111	**1.12**	1.66	1.05
	5(1)[b]	300	300	200	168	38.4	507	0.61	327	84	0.36	0.86	1.25
	5(2)[c]	300	300	200	168	38.4	507	0.60	234	86	**1.10**	1.86	1.00
Sherif & Dilger (2000a,b) Continuous	S1-2	250	250	150	114	28.0	444	1.34	185	44	0.38	0.80	1.11
	EC1(T2)	250	250	150	114	84.1	532	1.61	245	103	0.76	1.08	0.96

Note: a) (1) denotes end 1 and (2) end 2 of continuous slab, b) y = 150 mm, c) y = 0 mm and d) $\rho = \sqrt{\rho_l \rho_t}$

Table 1: Edge column tests without shear reinforcement

List of Figures

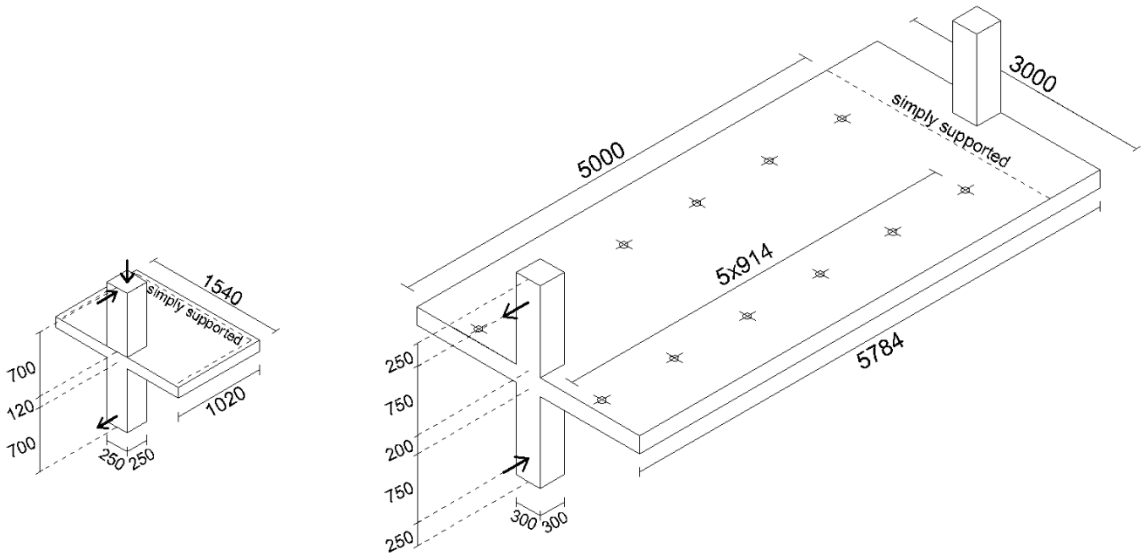

Figure 1: Geometry and loading arrangement of a) isolated slabs of El-Salakawy et al (1998) and b) continuous slabs of Regan (1993).

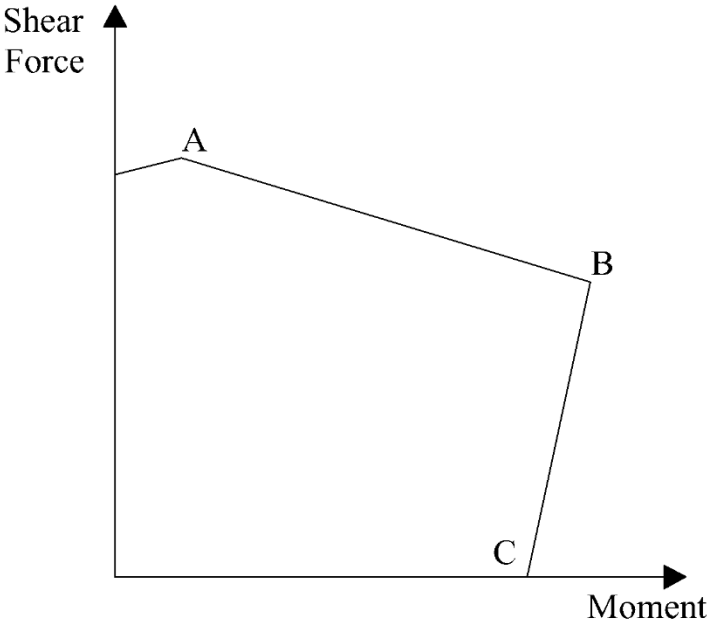

Figure 2: Interaction between punching resistance and unbalanced moment.

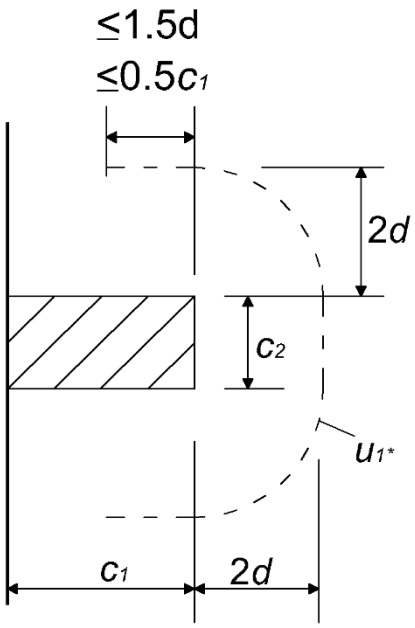

Figure 3: Reduced control perimeter of EC2

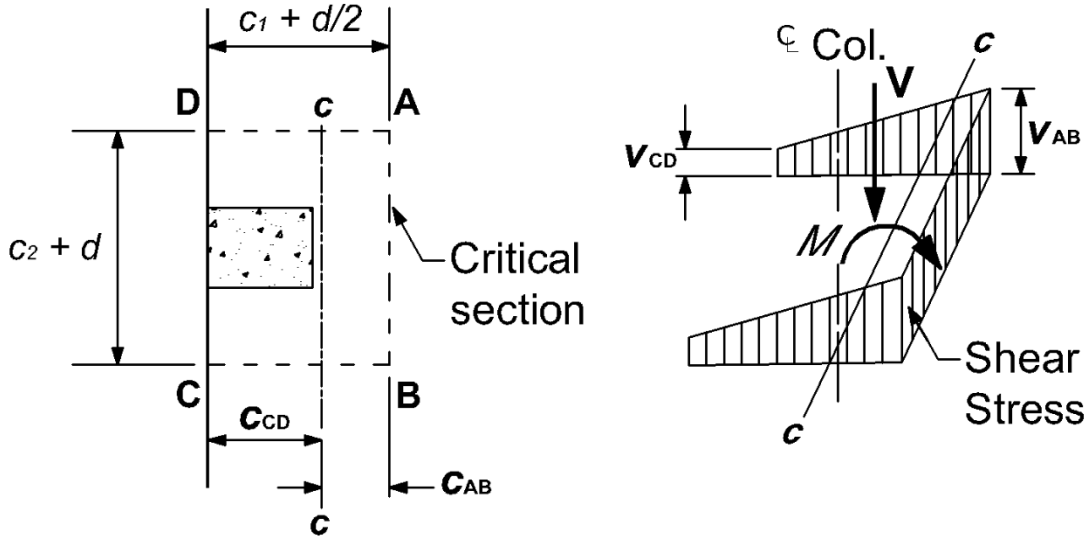

Figure 4: Critical perimeter of ACI 318 and corresponding shear stress distribution.

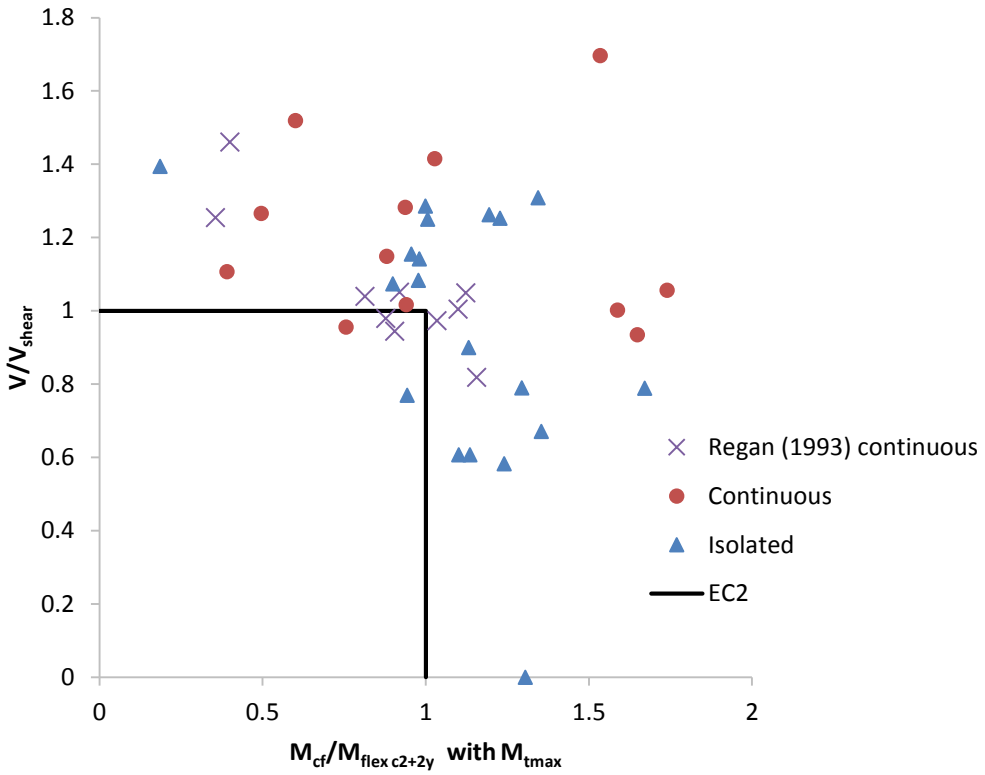

Figure 5: Interaction between punching resistance and unbalanced moment at column face for specimens in Table 1 with M_{flex} calculated using effective width of c_2+2y with $M_{flex} \leq M_{tmax}$.

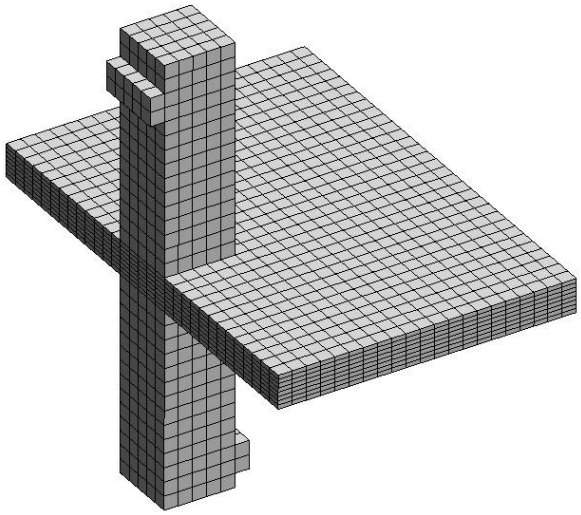

Figure 6: Finite element mesh used for analysis of slabs of El-Salakawy et al (1998)

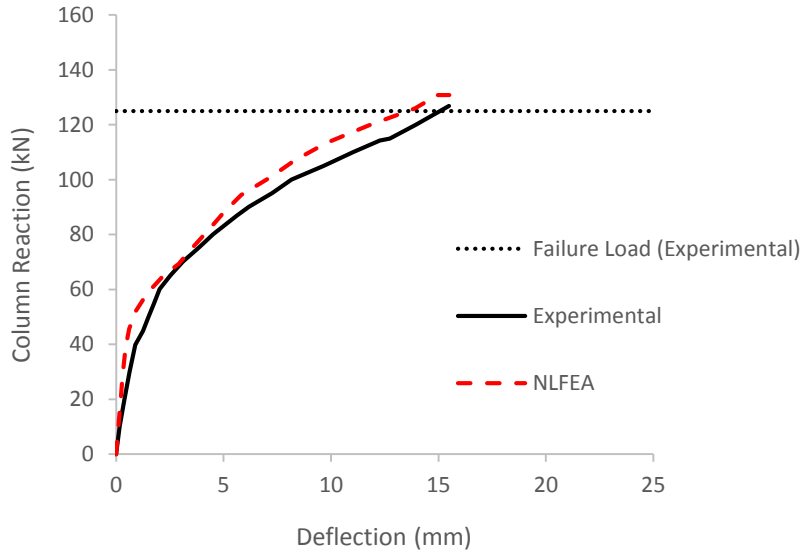

Figure 7: Comparison of measured and predicted deflections for slab XXX (El-Salakawy et al, 1998)

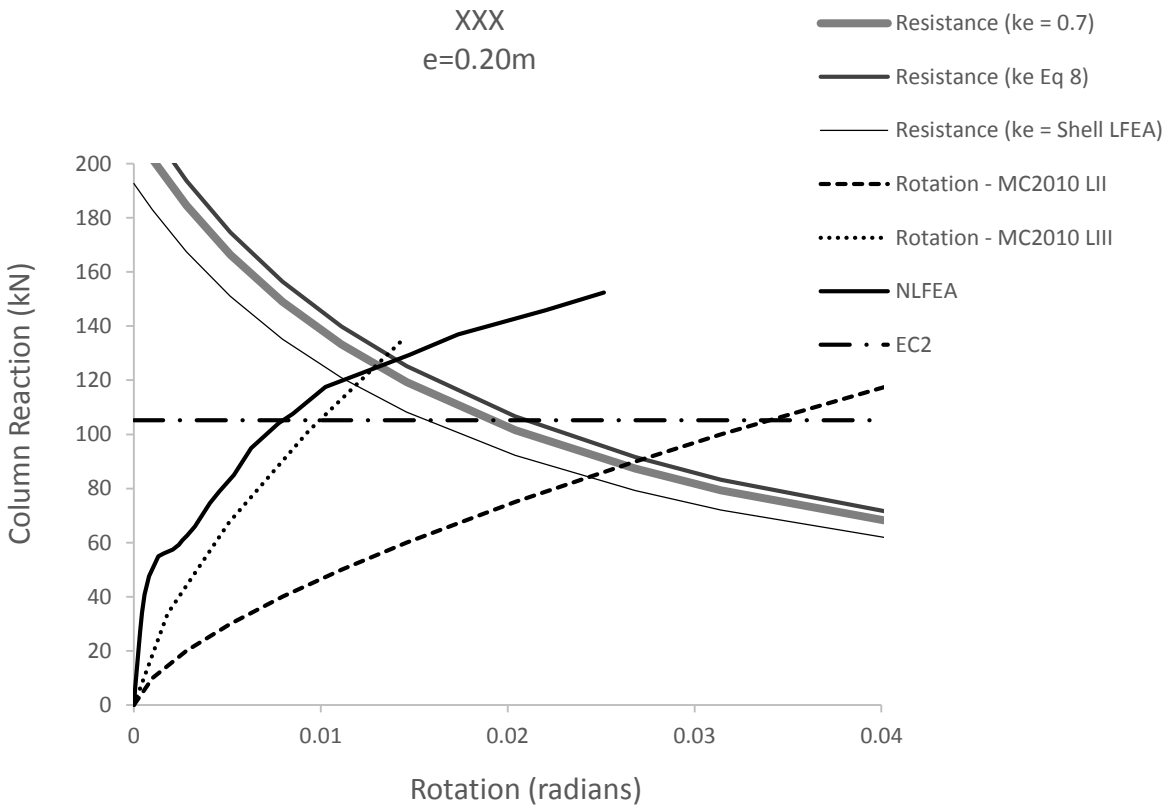

a)

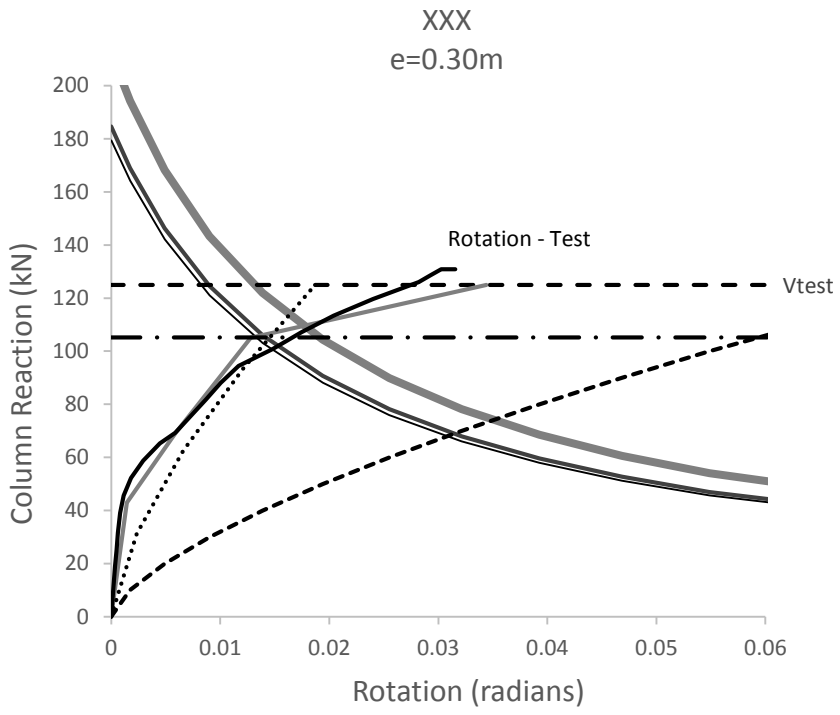
XXX
e=0.30m
Column Reaction (kN)
Rotation (radians)
Rotation - Test
Vtest
0
20
40
60
80
100
120
140
160
180
200
0
0.01
0.02
0.03
0.04
0.05
0.06

b)

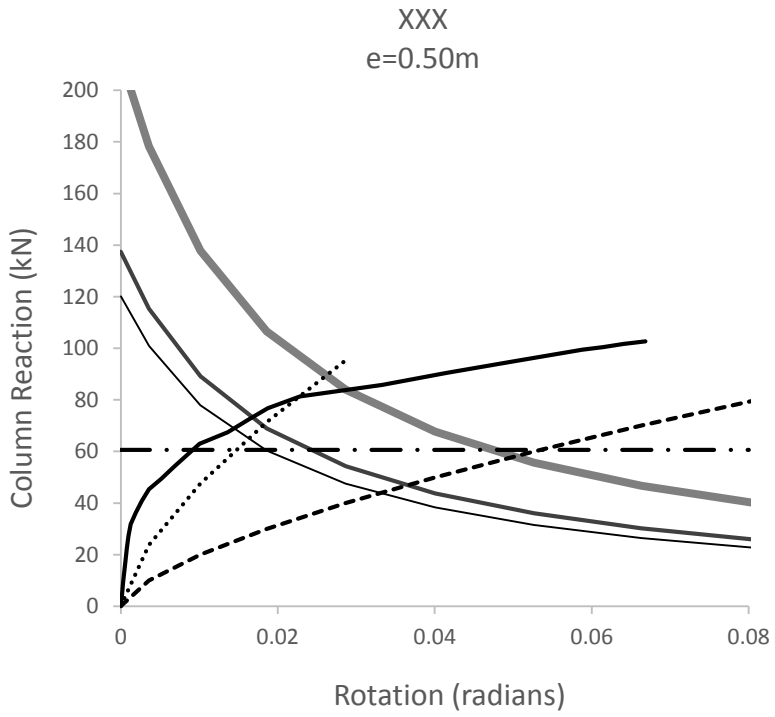
XXX
e=0.50m
Column Reaction (kN)
Rotation (radians)
0
20
40
60
80
100
120
140
160
180
200
0
0.02
0.04
0.06
0.08

c)

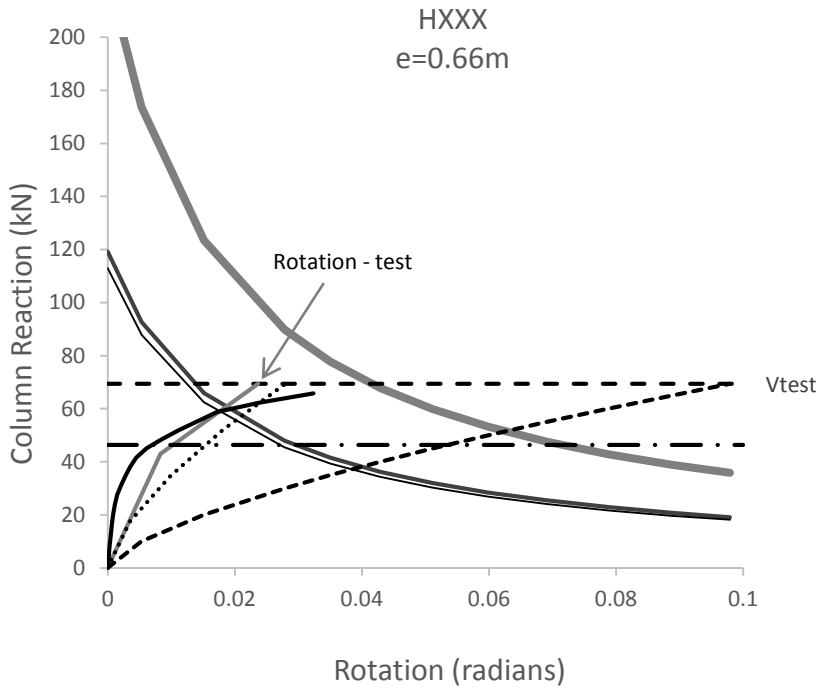

d)

Figure 8: Assessment of slabs of El-Salakawy et al (1998) with MC2010 for eccentricities of a) 0.2 m, b) 0.3 m (XXX), c) 0.5 m and d) 0.66 m (HXXX)

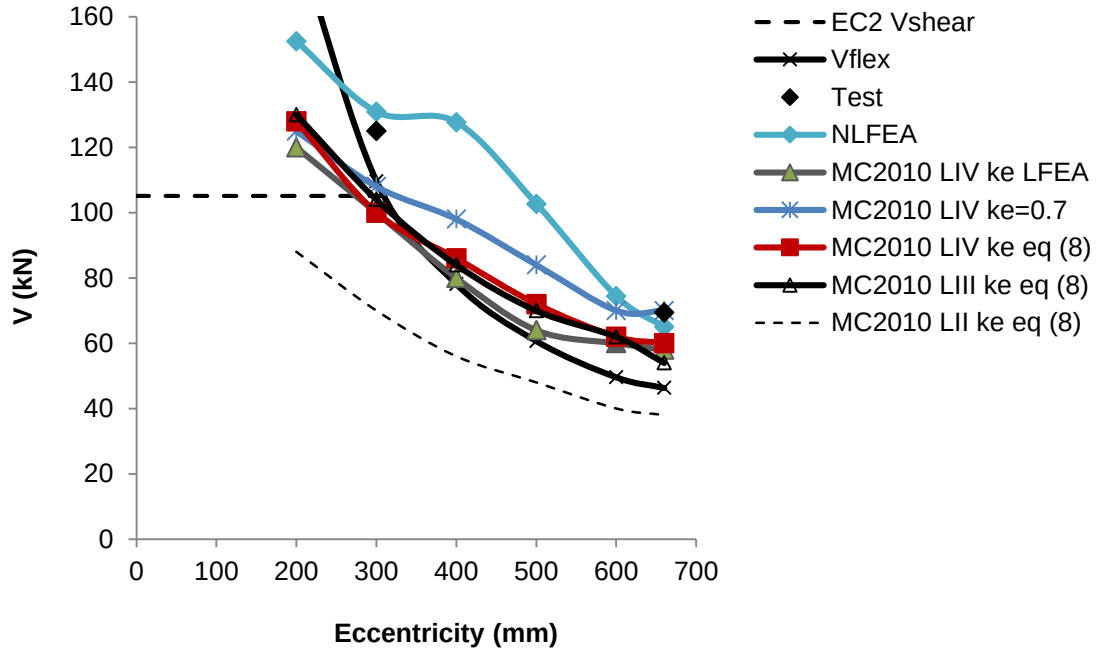

Figure 9: Influence of eccentricity on calculated punching resistance of slabs of El-Salakawy et al. (1998).

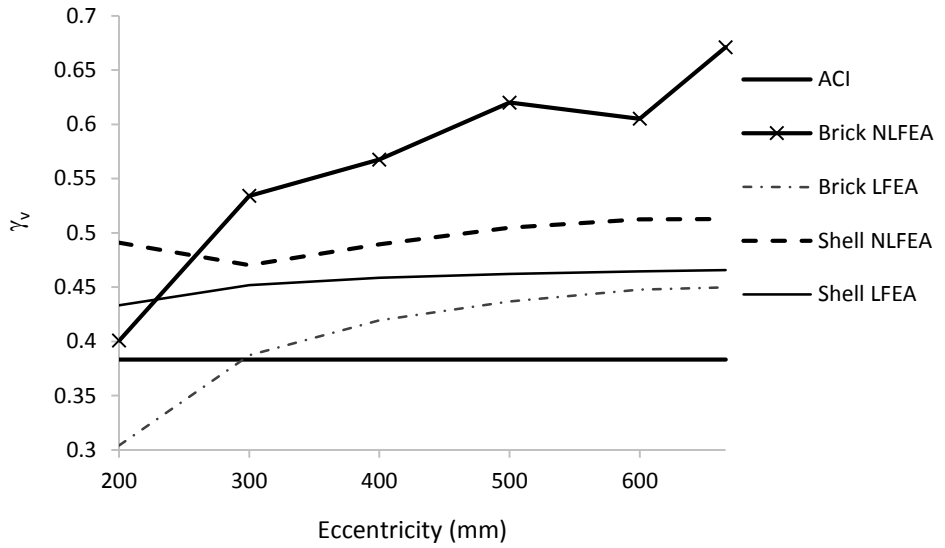
0.7
0.65
0.6
0.55
0.5
0.45
0.4
0.35
0.3
γv
200
300
400
500
600
Eccentricity (mm)
ACI
Brick NLFEA
Brick LFEA
Shell NLFEA
Shell LFEA

a)

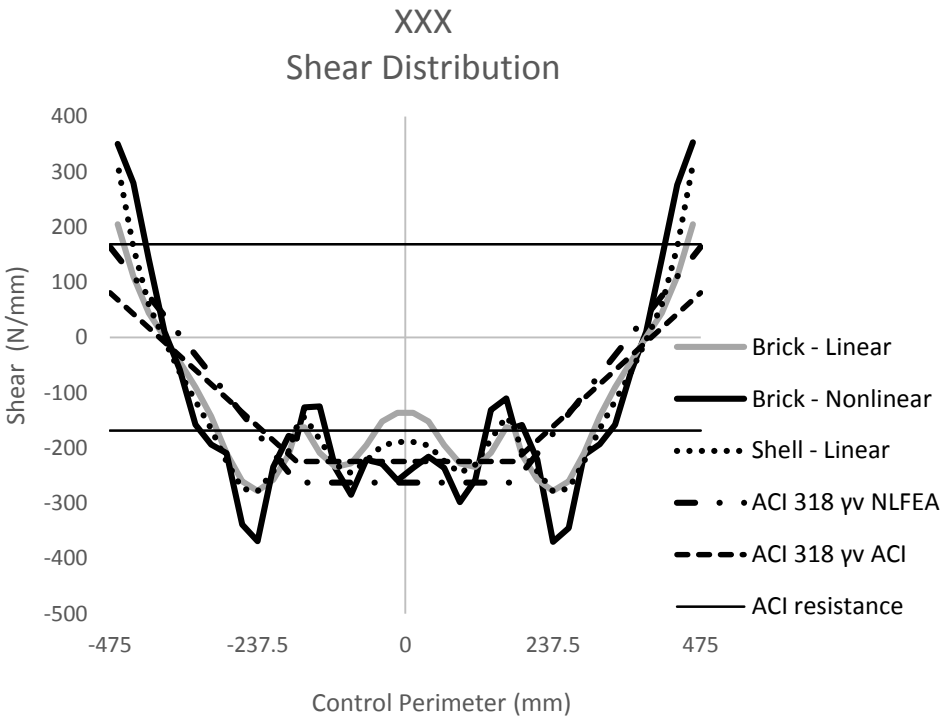
XXX
Shear Distribution
400
300
200
100
0
-100
-200
-300
-400
-500
Shear (N/mm)
-475
-237.5
0
237.5
475
Control Perimeter (mm)
Brick - Linear
Brick - Nonlinear
Shell - Linear
ACI 318 γv NLFEA
ACI 318 γv ACI
ACI resistance

b)

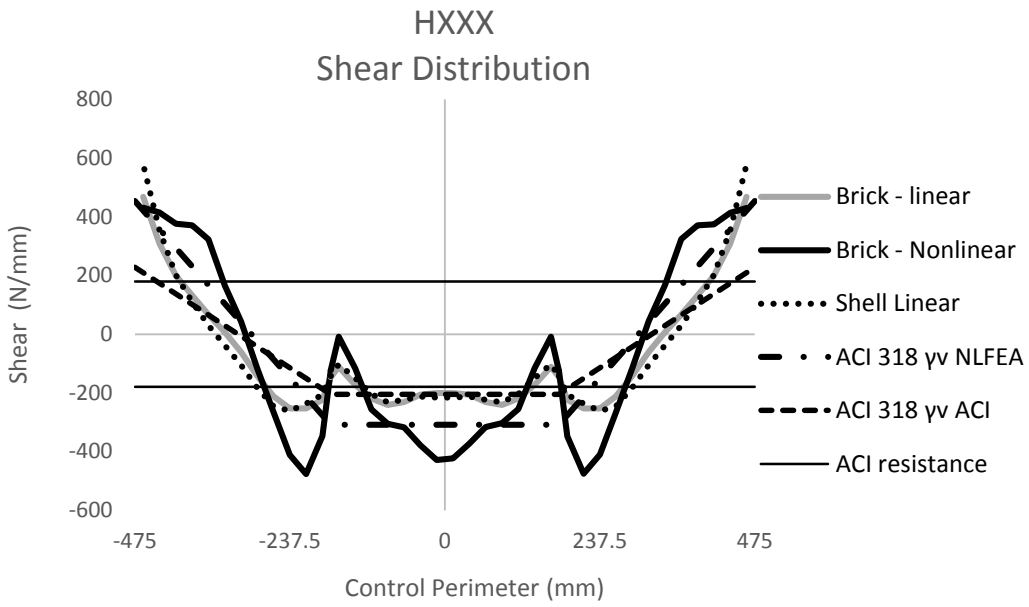

c)

Figure 10: Analysis of shear force distribution on ACI 318 critical perimeter for slabs of El-Salakawy et al. (1998) a) influence of eccentricity on γ_v for XXX, b) shear force distribution for XXX and c) shear force distribution for HXXX.

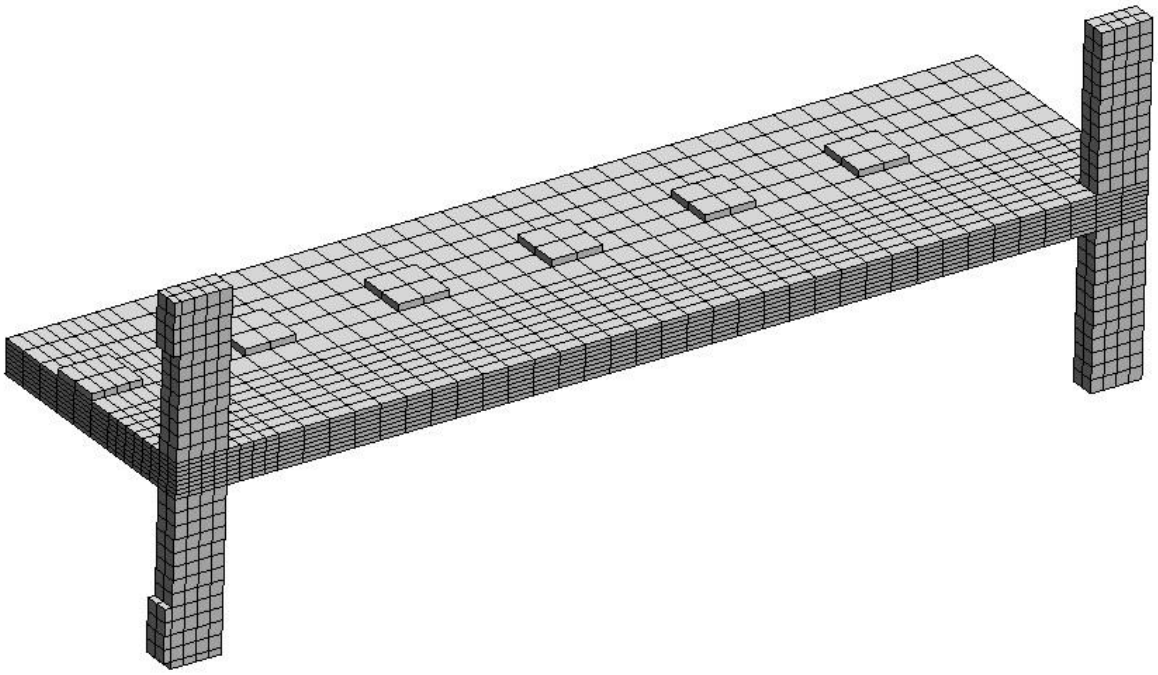

Figure 11: Finite element mesh used for slabs of Regan (1993).

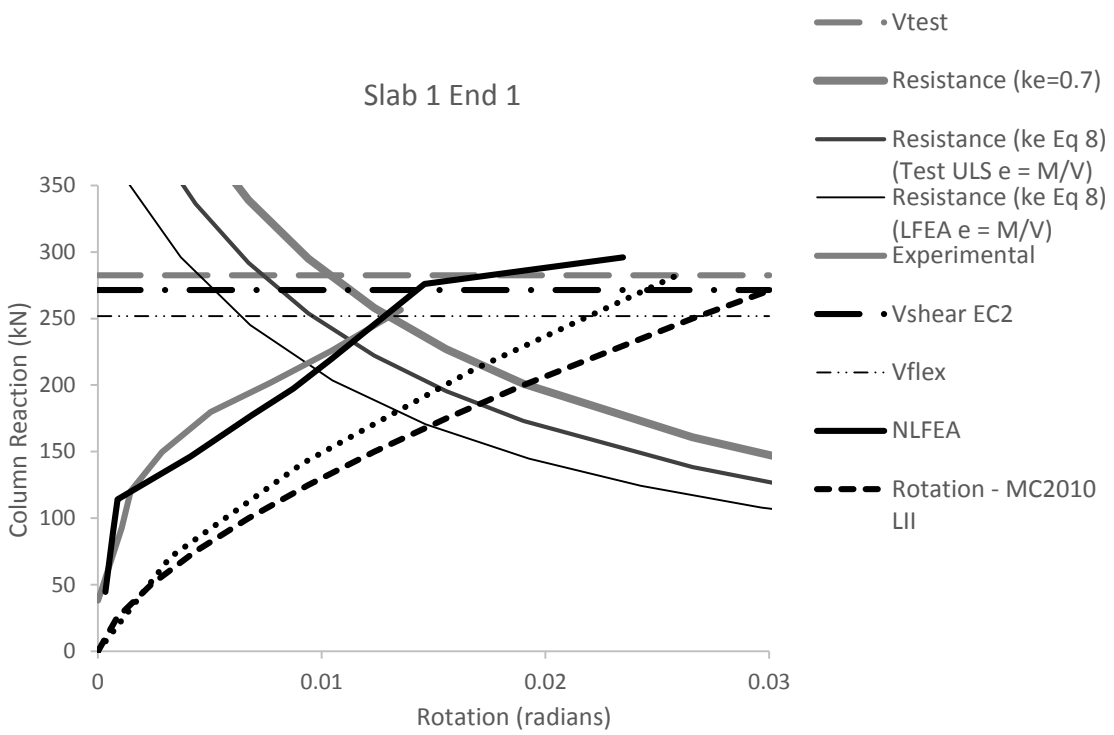
Slab 1 End 1
Column Reaction (kN)
Rotation (radians)
0
50
100
150
200
250
300
350
0
0.01
0.02
0.03
Vtest
Resistance (ke=0.7)
Resistance (ke Eq 8) (Test ULS e = M/V)
Resistance (ke Eq 8) (LFEA e = M/V)
Experimental
Vshear EC2
Vflex
NLFEA
Rotation - MC2010 LII

a)

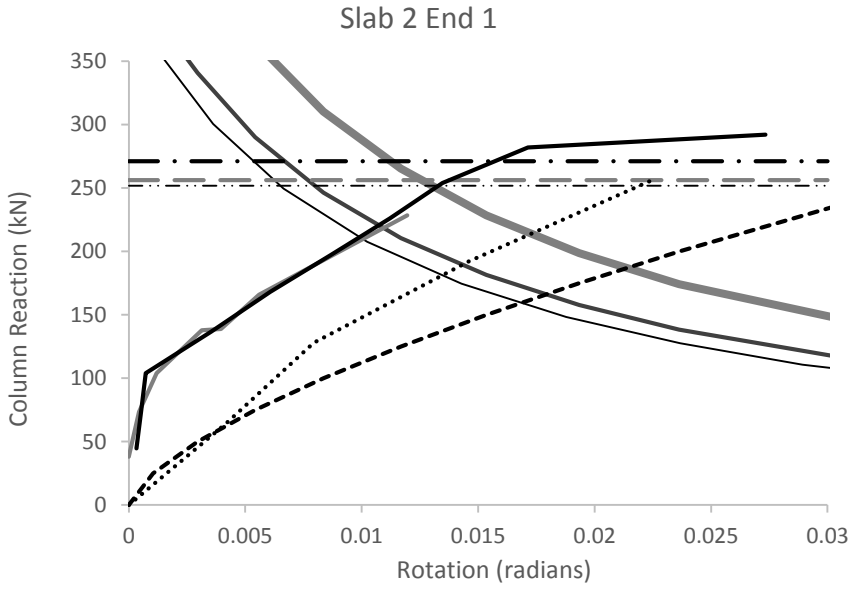
Slab 2 End 1
Column Reaction (kN)
Rotation (radians)
0
50
100
150
200
250
300
350
0
0.005
0.01
0.015
0.02
0.025
0.03

b)

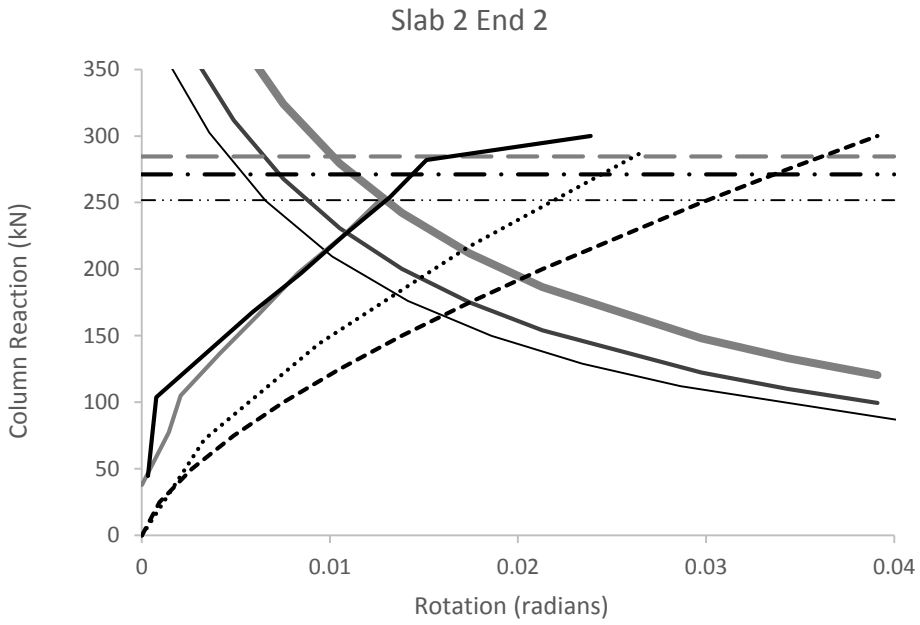
Slab 2 End 2
Column Reaction (kN)
350
300
250
200
150
100
50
0
0
0.01
0.02
0.03
0.04
Rotation (radians)

c)

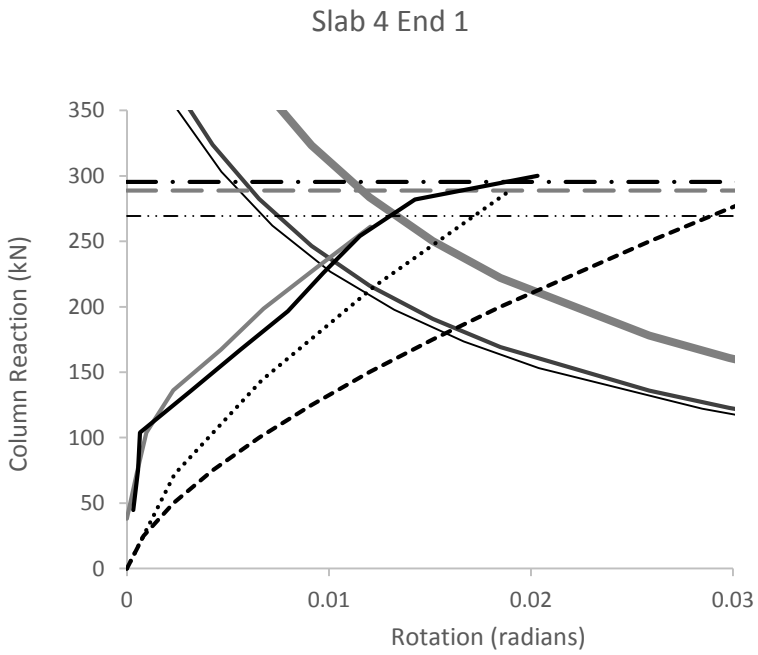
Slab 4 End 1
Column Reaction (kN)
350
300
250
200
150
100
50
0
0
0.01
0.02
0.03
Rotation (radians)

d)

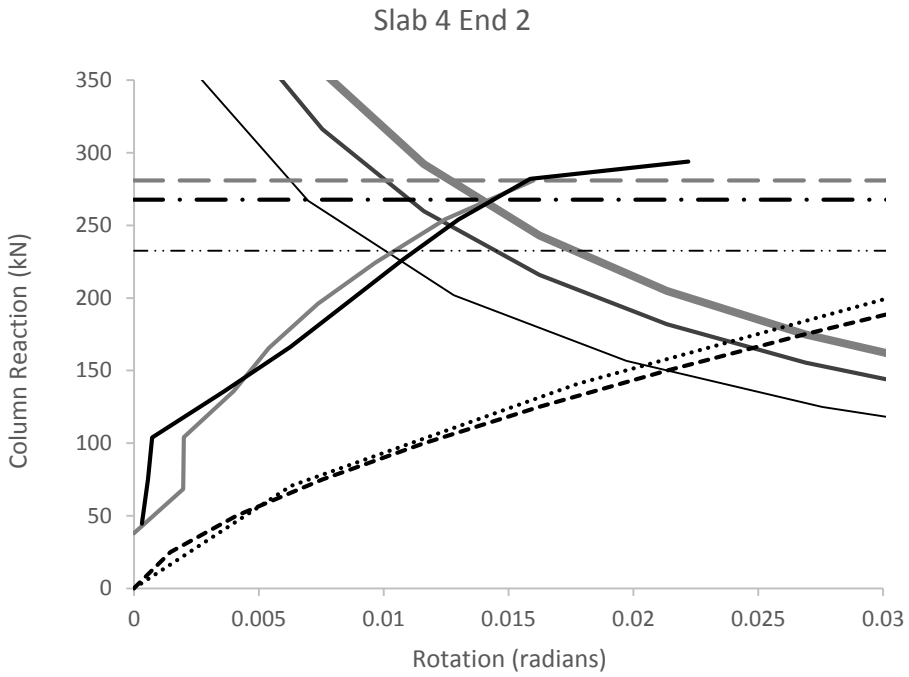

e)

Figure 12: Assessment of slabs of Regan (1993) with MC2010 for a) Slab 1 end 1, b) Slab 2 end 1, c) Slab 2 end 2, d) Slab 4 end 1 and e) Slab 4 end 2.

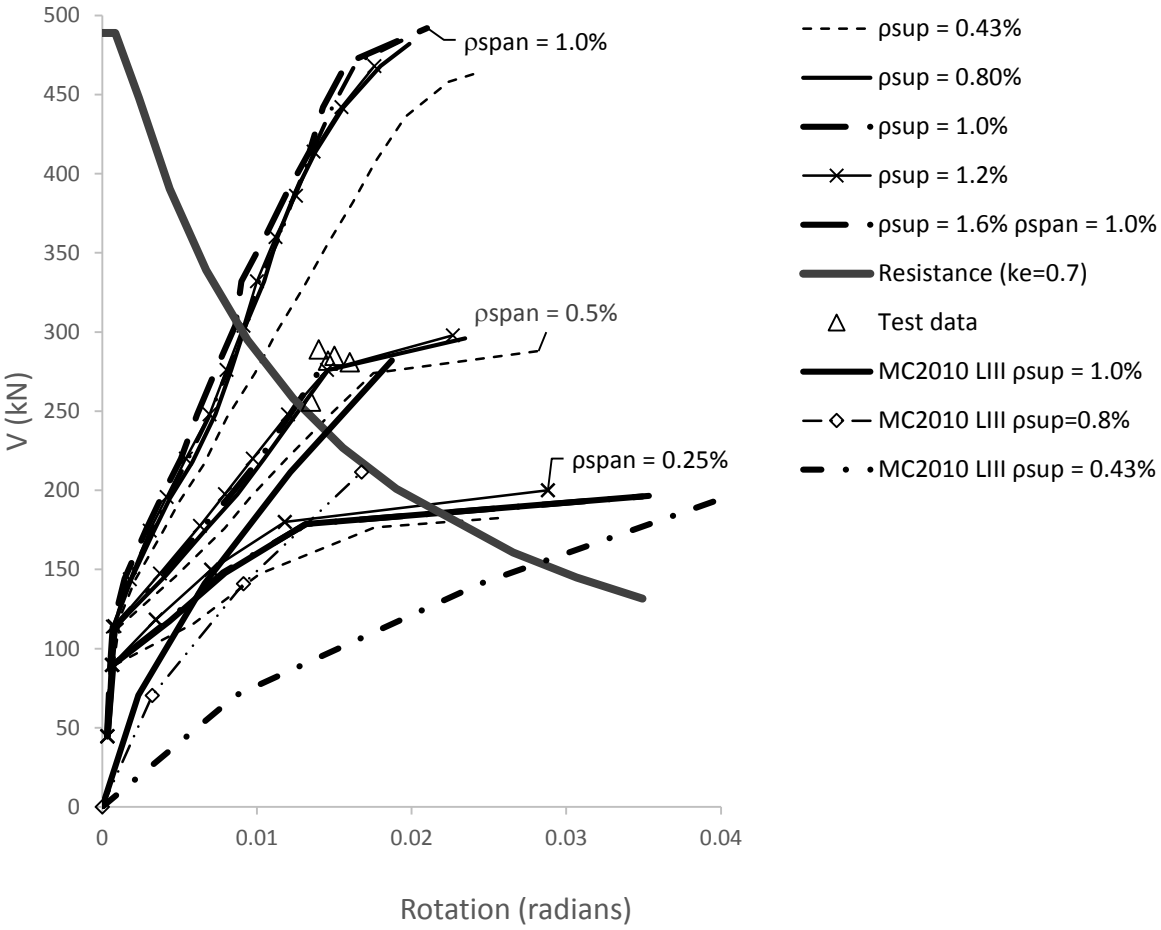
500
450
400
350
300
250
200
150
100
50
0
V (kN)
0
0.01
0.02
0.03
0.04
Rotation (radians)
ρspan = 1.0%
ρspan = 0.5%
ρspan = 0.25%
ρsup = 0.43%
ρsup = 0.80%
•ρsup = 1.0%
ρsup = 1.2%
•ρsup = 1.6% ρspan = 1.0%
Resistance (ke=0.7)
Test data
MC2010 LIII ρsup = 1.0%
MC2010 LIII ρsup=0.8%
•MC2010 LIII ρsup = 0.43%

a)

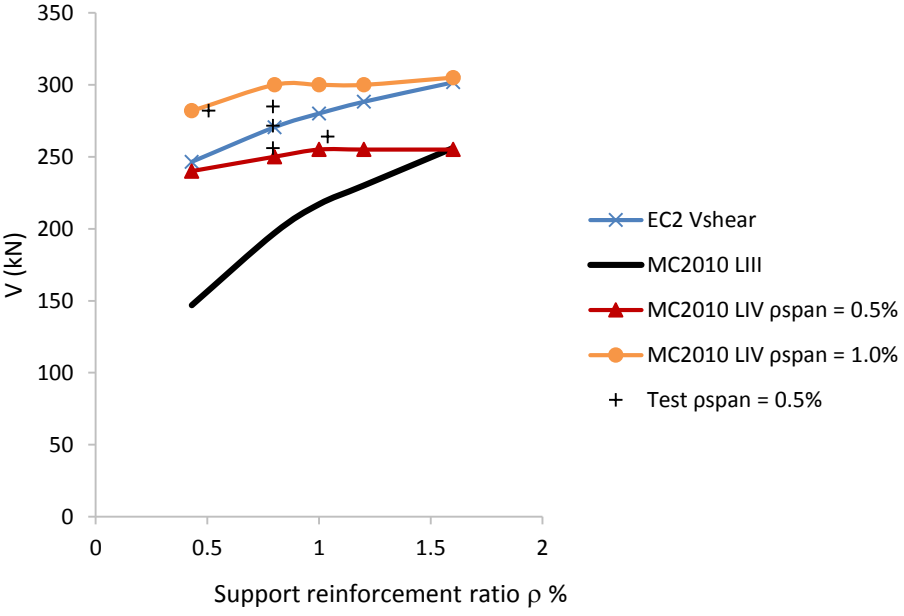
350
300
250
200
150
100
50
0
V (kN)
0
0.5
1
1.5
2
Support reinforcement ratio ρ %
EC2 Vshear
MC2010 LIII
MC2010 LIV ρspan = 0.5%
MC2010 LIV ρspan = 1.0%
Test ρspan = 0.5%

b)

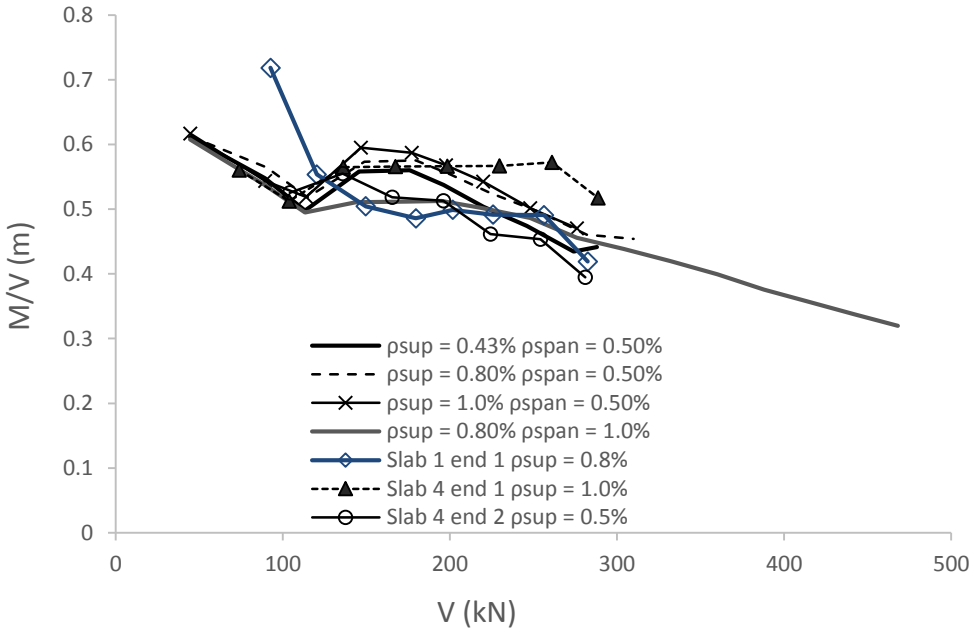

c)

Figure 13: Influence of varying reinforcement arrangement in Regan Slab 1 on a) rotation, b) punching resistance, c) M/V